Two decades of land cover changes in the Colombian Andes

Paulo Arévalo[1]
Ana Reboredo Segovia[2]
Christoph Nolte[1]

[1]Department of Earth and Environment, Center for Remote Sensing. Boston University, Boston, MA. 02445, USA.
[2]World Resources Institute, Washington, DC 20002, USA.

Correspondence to: Paulo Arévalo (parevalo@bu.edu)

Abstract

The Colombian Andes faces severe anthropogenic pressures from deforestation, agricultural expansion, mining, and urban development. Given its status as one of the world's biodiversity hotspot, land cover monitoring for effective conservation strategies and sustainable development planning is essential. While early research relied on coarse or medium-resolution satellite imagery for limited temporal coverage, recent initiatives like MapBiomas Colombia have improved national-scale mapping capabilities. However, mapping the complex spectral-temporal patterns of heterogeneous tropical mountain environments benefits from advanced methods that can track long-term surface trends. This study presents comprehensive annual land cover maps for the Colombian Andes and Sierra Nevada of Santa Marta spanning 1997-2024, representing the longest and most detailed temporal analysis of this critical region to date. We employed the Continuous Change Detection and Classification (CCDC) algorithm applied to Landsat data, coupled with machine learning models trained on a custom dataset designed to address existing limitations in temporal depth and spatial detail. Our time series approach leverages spectral-temporal signatures to distinguish land cover types with similar spectral characteristics but

distinct temporal behaviors, providing a unique method for monitoring forest dynamics, habitat changes, and anthropogenic impacts across the Colombian Andes.

1. Introduction

The tropical Andes constitute one of the world's biodiversity hotspots in terms of species richness and endemism [1]. Forests in this region are important for habitat provision, carbon sequestration, water regulation, landslide prevention, and climate change adaptation. The Colombian Andes are home to approximately 78% of Colombia's population and to the largest percentage of endemic species in the country [2]. However, the Colombian Andes have been substantially transformed due to anthropogenic pressures from deforestation, agricultural expansion, mining, and urban development. Many threatened species are confined to substantially reduced forest habitats and small ranges that will likely shift and contract with climate change [3,4]. Accurate land cover monitoring is therefore essential for evidence-based conservation strategies, sustainable development planning, and compliance with international environmental agreements, including the Convention on Biological Diversity and REDD+ mechanisms.

Early research efforts covering the entire study area focused on forest cover assessment using coarse-resolution satellite imagery [5,6], or medium-resolution for one or a few anniversary epochs [7,8]. More recent work has investigated forest change dynamics [9], land use and land cover [10,11], change detection [12] and drivers of forest disturbance [13] in the area. However, those studies have been conducted at very local scales (subregional or municipal scales). Efforts with higher spatial and temporal coverage include the MapBiomas Colombia initiative, which generates annual land cover maps for the entire country from 1985 to present using cloud processing and automated classifiers (MapBiomas Colombia, 2024), and the national, official forest cover and forest loss reports, generated annually by the Institute of Hydrology, Meteorology and Environmental Studies of Colombia [14].

Time series algorithms offer substantial advantages over traditional mapping methods for complex landscapes. The spectral-temporal patterns captured by them aid in the separation of land cover types that exhibit similar spectral characteristics but distinct temporal behaviors. Time series algorithms such as the Continuous Change Detection and Classification algorithm (CCDC) or BFAST [15,16] can model the complex temporal signatures that can arise in heterogeneous tropical mountain environments, where vegetation varies significantly across elevation gradients and microclimatic conditions.

This study presents high-quality annual land cover maps for the Colombian Andes and the Sierra Nevada of Santa Marta, covering the temporal range between 1997-2024. The maps have been generated using the outputs of the CCDC algorithm applied to Landsat data, and a machine learning model training using a custom dataset compiled to address existing limitations and provide great temporal depth and spatial detail. We assess the accuracy of the maps and estimate stable and change areas using a stratification generated between 2012-2024, coinciding with the era of high-resolution imagery.

2. Methods

2.1 Study area

The study area encompasses the natural Andean region of Colombia, plus the municipalities connecting it to the Sierra Nevada of Santa Marta (Figure 1). The Andean region has the highest population density in the country, resulting in extensive historical conversion of original forest cover to human-dominated landscapes such as agricultural fields, grazing lands, planted forests, and built infrastructure [17–19]. The Andean region is rich in threatened and endemic species (CITE) , while the Sierra Nevada is considered the most irreplaceable protected area in the world for threatened species [20]. Forest fragmentation is widespread throughout the study area region, but substantial intact forest blocks remain, particularly on the Pacific coast and in the eastern slopes of the eastern mountain range [21].

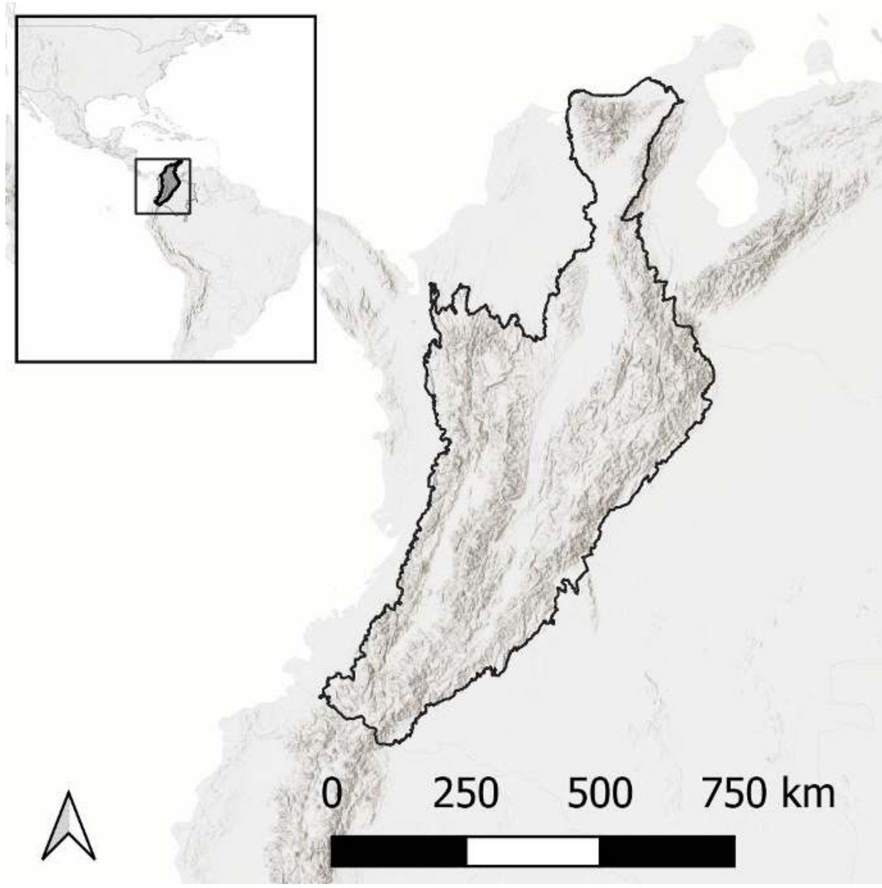

Figure 1. Study area, which includes the Andean region of Colombia and Sierra Nevada of Santa Marta municipalities. Basemap attribution: Esri, Maxar, Airbus DS, USGS, NGA, NASA, CGIAR, N Robinson, NCEAS, NLS, OS, NMA, Geodatastyrelsen, Rijkswaterstaat, GSA, Geoland, FEMA, Intermap, and the GIS user community.

2.2 Training dataset

We generated a training dataset containing labels for the following classes: natural forest, planted forest, developed, pasture/agriculture, water, barren, and oil palm. Training data for all classes except plantations and oil palm was generated through a mix of opportunistic collection and a sample generated from a vector land cover map available for the Andes generated by visual interpretation by the multiple official research institutes in Colombia for the year 2009-2010 [22]. Additional data was also supplemented from[23]. Training data for oil palm and forest plantations was collected manually, using high resolution imagery from Google Earth, ESRI Wayback and Planet basemaps, as well as the time series of Landsat-derived indices and bands (when required). The training dataset distribution disaggregated by year is shown in Figure 2. The unbalanced distribution mirrors the class distribution in the study area.

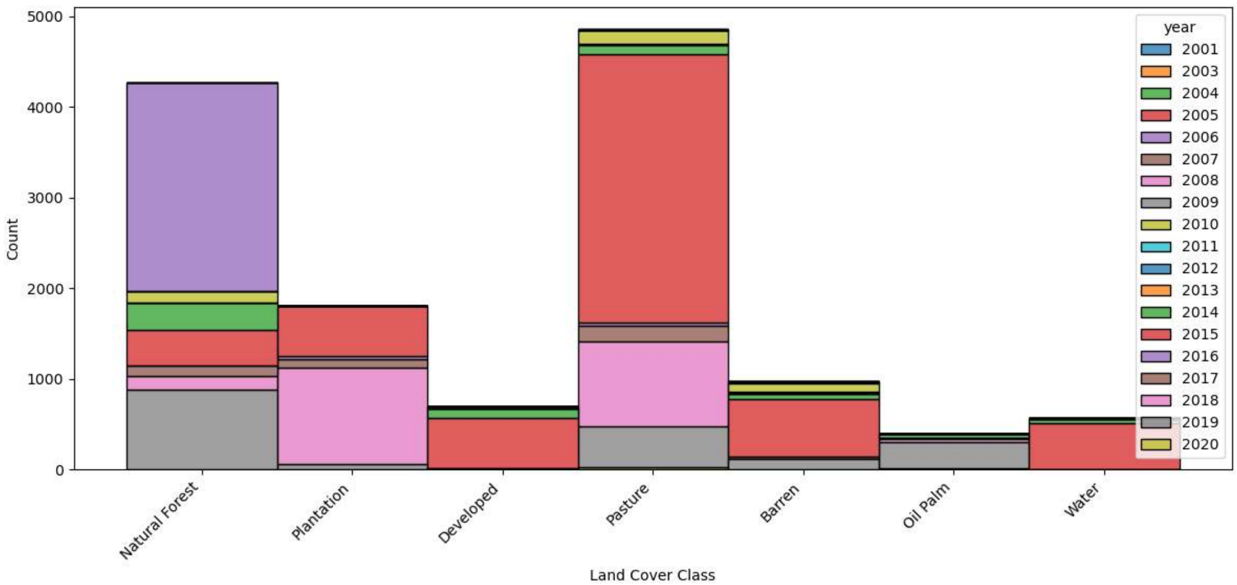

Figure 2. Training data histogram, disaggregated by year. Most training points were collected for recent years, for which high-resolution imagery is available.

2.3 Land cover classification

We trained a random forest model [24] with the training dataset described above to predict annual land cover classes in probability mode using predictor variables derived from the Continuous Change Detection and Classification (CCDC) algorithm [15]. We ran CCDC on a 25-year (1997-2022) time-series stack of Landsat Collection 2-derived data including: surface reflectance and unmixed spectral components. We filtered surface reflectance data to remove low-quality pixels, including pixels with radiometric saturation, clouds or cloud shadows, and high atmospheric opacity. We then derived the unmixed spectral components from the filtered images. The use of spectral unmixing [25] allowed us to obtain fractional abundances of green vegetation (GV), non-photosynthetic vegetation (NPV), soil and shade per pixel, and with those, the Normalized Difference Fraction Index, which can be useful to detect subtle forest disturbances. In addition to the intercept (INTP) and slope (SLP) of the time segments, we used the first two harmonics, transformed to phases and amplitudes, as well as the segment Root-Mean-Square-Error (RMSE) and synthetic (SYNT) reflectance computed for the first of July of each year. The final predictors used, including additional ancillary data, are shown in Table 1.

Table 1. Predictors used for the random forest model. Sources: topographic variables [26], Water occurrence [27], world settlement footprint [28].

BAND TYPE	BAND NAME	CCDC COEFFICIENTS AND DERIVATIVES (Generated for every single band)
Surface reflectance	GREEN, RED, NIR, SWIR1, SWIR2	INTP, SLP, PHASE, PHASE2 AMPLITUDE, AMPLITUDE2 RMSE, SYNT
Index or transform	NDFI	
Unmixed spectral components	Shade	
Other variables	ELEVATION, ASPECT, DEM_SLOPE, WATER OCCURRENCE, WORLD SETTLEMENT FOOTPRINT	

2.4 Post-processing

Given the complexity of the landscape in our study area and the spectral-temporal similarity between some vegetation classes, we followed the classification protocol used for the Global Land Cover Maping and Estimation (GlanCE) product [29,30]. This protocol can be summarized in the following steps:

1. A temporal consistency enhancement similar to that implemented by the Land Change Monitoring, Assessment, and Projection (LCMAP) initiative [31,32] in which class probabilities are averaged across all years for each stable CCDC segment, and the class with highest average probability is assigned to represent the dominant land cover for that segment. In turn, CDCDC segments that show signs of being in a transitional state (e.g.

conversion from one vegetation class to another) are identified and processed to improve the label assignment in the first and second halves of the segments. Missing values between CCDC segments are filled using temporal interpolation of the labels, resulting in continuous labels for the entire study period.

2. A post-processing step to identify omission of forest loss mapping, in which pixels where CCDC detected a break, but the land cover sequence did not show evidence of it are flagged and corrected, using rules that include the magnitude or change and the shift in class probabilities over time.
3. A set of final post-processing steps that address specific issues, such as improbable labels (e.g. water in high slopes, barren in areas that green up regularly, or in areas with permanent water cover), correcting them with more plausible labels or transitions.

In addition to the GLanCE mapping protocol, we removed patches equal to or less than 1 ha, replacing the class labels as follows: for oil palm, we picked the second most likely vegetation class; for developed, the second most likely class among all possible classes; and for tree plantation classes, the second most likely class of either the natural forest or pasture classes. Finally, we removed pixels with less than 29 clear observations (as reported by the CCDC algorithm), which is equivalent to approximately only one observation per year, because those were considered low quality. Those pixels correspond predominantly to very high elevation locations with almost permanent cloud cover.

2.5 Stratification, strata adjustment and

A final post-processing step was applied after deriving the final stratification used to assess the dataset accuracy. The strata layer was generated for the period 2012 - 2024 (Table 2), coinciding with the era of the best high-resolution imagery availability on Google Earth and Esri Wayback. This choice was necessary because the interpretation of the reference samples required for accuracy assessment and area estimation is highly unreliable when no high-resolution imagery is available.

A preliminary accuracy assessment conducted on a previous iteration of the land cover datasets had revealed excessive change from pasture/ag into other classes, and overprediction of planted forest. We used the transition probabilities from that map to derive the transition matrix to parameterize a Hidden Markov Model (HMM, similar to [33]) but modified it to address those issues by increasing the probability of pasture/ag remaining stable, and increasing the change probabilities from planted forest. After implementing those changes, we applied the HMM only over the strata pixels labelled as *planted forest*, *forest loss 2*, and *forest gain*, replacing the entire sequence of labels for the entire study period with those indicated by the HMM. With those modified labels, we re-generated the final stratification used for the accuracy assessment, resulting in the class proportions shown in Table 2.

2.6 Sampling and response design

A stratified design and estimation approach was implemented [34,35], with the stratified random sample (n=1960) targeting stable and change classes. The sampling assessment unit was a 30 m × 30 m Landsat pixel, which was chosen to coincide with the minimum mapping unit. A buffer class was included to minimize the negative effects of forest loss omission [36,37]. The sample unit allocation is shown in Table 2.

Table 2. Stratification for 2012 - 2024. Any changes not described below were assigned the class “Other changes”, class number 13. Class weights (Wh) computed from the final stratification map. Sample units (n) allocated per stratum.

Stratum name	**Description**	**Class number**	**Wh**	**n**
Stable Natural forest	PENDING	1	0.323	560
Stable Planted forest		2	0.002	40
Stable Developed		3	0.006	40
Stable Pasture / Ag		5	0.418	730
Stable Water		6	0.007	40
Stable Barren		7	0.008	40
Stable Oil Palm		8	0.003	40
Forest loss 1	Natural forest to Pasture/Ag	9	0.025	60
Forest loss 2	Natural forest to Oil palm | plantation	10	0.001	40
Forest gain	Pasture/Ag to Natural or planted forest	11	0.016	40

Buffer class	1 pixel from other classes into Natural Forest	12	0.182	300
Other	Other changes not described above	13	0.008	30

Reference observations for the range 2012 - 2024 were provided by each sample unit by examining high resolution imagery (Google Earth, ESRI Wayback, Planet-NICFI basemaps), as well as time series of Landsat Collection 2 surface reflectance observations, NDFI and NDVI time series for the range between 2010 and 2024. All the points mapped or referenced as change classes were cross-checked, as well as any labels assigned a *low* confidence in the interpretation.

3. Results

A map showing the stratification (stable and change classes) for 2012-2024 is shown in Figure 3.

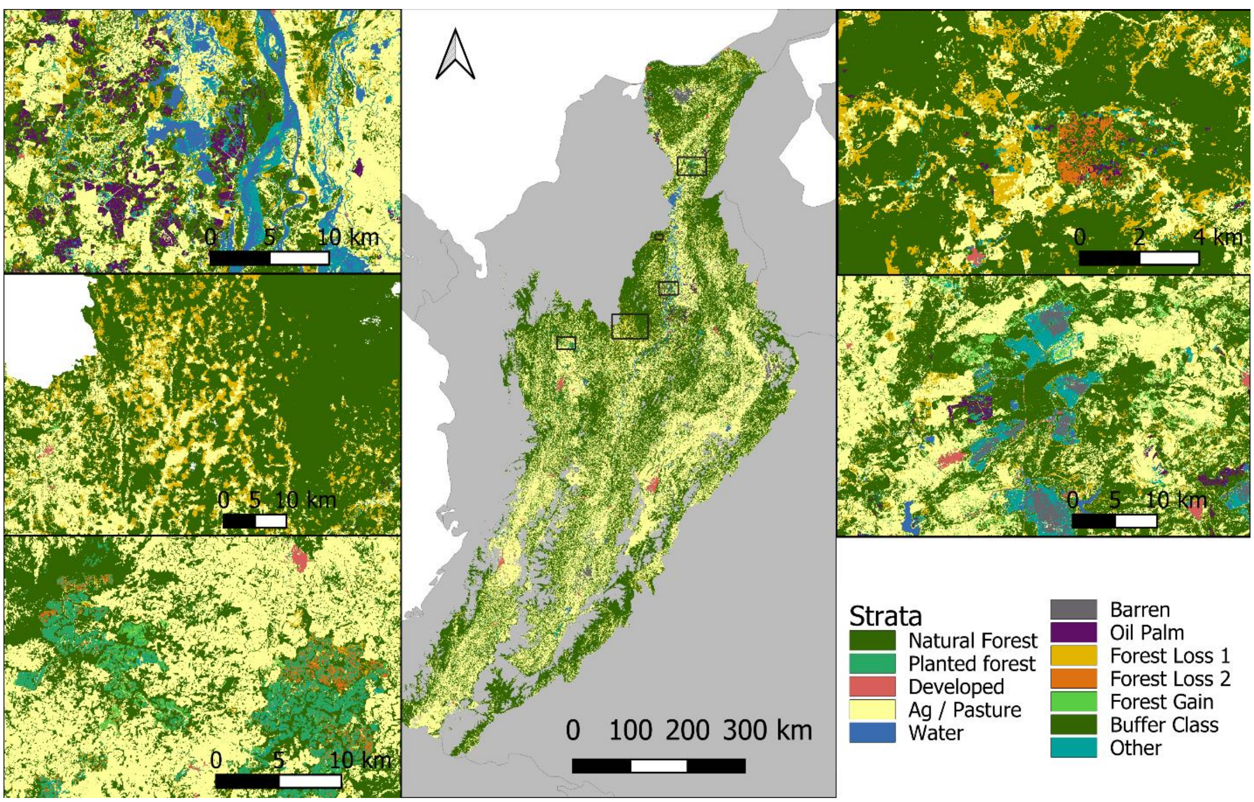

Figure 3. Stratification for 2012-2024, showing five examples of change: a) multiple changes in a complex landscape, b) forest loss, c) stable and new plantations, d) PENDING, e) stable and new mining.

The confusion matrix derived from the reference sample, and accuracies for the final stratification layer are shown in Table 3. Overall accuracy is 0.791. The mapped and estimated areas with 95% confidence intervals are shown in Table 4.

Table 3. Confusion matrix with counts, for the strata classes described in Table 2. Reference labels are in columns, strata classes in rows. *Wh* represents the mapped strata proportions, while *props* represents the estimated class proportions.

	1	**2**	**3**	**5**	**6**	**7**	**8**	**9**	**10**	**11**	**12**	**13**	***Total***	***Wh***
1	519	4	0	27	0	0	1	3	0	6	0	0	*560*	0.323
2	6	28	0	0	2	0	0	0	0	2	0	2	*40*	0.002
3	3	0	31	3	0	0	0	0	0	0	0	3	*40*	0.006
5	107	1	5	590	2	9	1	1	0	7	0	7	*730*	0.418
6	1	0	0	2	36	1	0	0	0	0	0	0	*40*	0.007
7	0	0	0	17	0	23	0	0	0	0	0	0	*40*	0.008
8	1	1	0	1	0	0	37	0	0	0	0	0	*40*	0.003
9	8	0	0	13	1	0	0	36	1	0	0	1	*60*	0.025
10	11	10	0	2	0	0	7	0	3	4	0	4	*41*	0.001
11	15	2	0	11	0	0	0	1	0	9	0	2	*40*	0.016
12	0	20	0	72	3	3	4	3	0	6	186	3	*300*	0.182
13	1	2	0	6	9	1	5	0	0	0	0	6	*30*	0.008
Total	*672*	*68*	*36*	*744*	*53*	*37*	*55*	*44*	*4*	*34*	*186*	*28*	*1961*	
Props	*0.372*	*0.018*	*0.008*	*0.413*	*0.012*	*0.012*	*0.008*	*0.020*	*0.001*	*0.015*	*0.113*	*0.009*		
User's acc.	0.927	0.700	0.775	0.808	0.900	0.575	0.925	0.600	0.073	0.225	0.620	0.200		
Prod. Acc.	0.805	0.078	0.625	0.818	0.537	0.386	0.347	0.770	0.175	0.244	1.000	0.165		
Overall acc.	0.791													

Table 4. Estimated areas, 95% confidence intervals, mapped areas and difference between mapped and estimated areas. Negative values in the map – estimate area column reflect classes that are under-represented in the stratification map. All areas are in ha.

	Est. area	CI area	Lower CI	Upper CI	Mapped area	Map – est. area
Stable Natural forest	11,154,044	397,608	10,756,436	11,551,652	9,692,167	-1,461,877
Stable Planted forest	544,328	176,934	367,394	721,262	60,597	-483,731
Stable Developed	229,127	78,934	150,193	308,061	184,749	-44,378
Stable Pasture / Ag	12,398,788	492,398	11,906,390	12,891,186	12,548,237	149,449
Stable Water	374,399	92,778	281,621	467,177	223,259	-151,140
Stable Barren	362,312	125,201	237,111	487,513	242,927	-119,386
Stable Oil Palm	232,675	91,544	141,132	324,219	87,376	-145,299
Forest loss 1	591,888	134,068	457,821	725,956	759,801	167,913
Forest loss 2	15,341	24,995	-9,654	40,337	36,601	21,259
Forest gain	449,846	162,385	287,461	612,232	487,335	37,489
Buffer class	3,392,176	301,020	3,091,156	3,693,196	5,471,251	2,079,076
Other	278,312	121,605	156,708	399,917	228,937	-49,375

4. Discussion

We present a land cover and land cover change datasets for the Andes region of Colombia, generated annually between 1997 to 2025. Our dataset is a comprehensive effort to characterize stable and change land cover classes in the area using a transparent, strong methodology.

Analize areas. All of them are valid, despite being tiny fractions of the entire study area

Previous results? While MapBiomas provides annual maps with high accuracy, their change accuracies are currently not reported. IDEAM data.

What results mean

Why are accuracies low for some classes

What can be done to improve the results?

5. Conclusion

6. Acknowledgements

This research was supported by the NASA Land-Cover and Land-Use Change program (grant 80NSSC20K1486, PI: Nolte). We thank Quinn Adamy and Al Hotimski for their careful work interpreting the reference sample, and Eric Bullock for his initial experiments with this work.

7. Bibliography

1. Myers, N.; Mittermeier, R.A.; Mittermeier, C.G.; da Fonseca, G.A.B.; Kent, J. Biodiversity Hotspots for Conservation Priorities. *Nature* **2000**, *403*, 853–858, doi:10.1038/35002501.
2. González, I.; Noguera-Urbano, E.A.; Velásquez-Tibatá, J.; Ochoa-Quintero, J.M. Especies Endémicas, Áreas Protegidas y Deforestación. In *Biodiversidad 2018. Estado y tendencias de la biodiversidad continental de Colombia.*; Moreno, L.A., Andrade, G. I, Gómez, M.F., Eds.; Instituto de Investigación de Recursos Biológicos Alexander von Humboldt.: Bogotá, D. C., Colombia., 2018.
3. Báez, S.; Jaramillo, L.; Cuesta, F.; Donoso, D.A. Effects of Climate Change on Andean Biodiversity: A Synthesis of Studies Published until 2015. *Neotropical Biodiversity* **2016**, *2*, 181–194, doi:10.1080/23766808.2016.1248710.
4. Velásquez-Tibatá, J.; Salaman, P.; Graham, C.H. Effects of Climate Change on Species Distribution, Community Structure, and Conservation of Birds in Protected Areas in Colombia. *Reg Environ Change* **2013**, *13*, 235–248, doi:10.1007/s10113-012-0329-y.
5. Etter, A.; McAlpine, C.; Phinn, S.; Pullar, D.; Possingham, H. Unplanned Land Clearing of Colombian Rainforests: Spreading like Disease? *Landscape and Urban Planning* **2006**, *77*, 240–254.
6. Sánchez-Cuervo, A.M.; Aide, T.M.; Clark, M.L.; Etter, A. Land Cover Change in Colombia: Surprising Forest Recovery Trends between 2001 and 2010. *PLOS ONE* **2012**, *7*, e43943, doi:10.1371/journal.pone.0043943.
7. González-González, A.; Clerici, N.; Quesada, B. A 30 M-Resolution Land Use-Land Cover Product for the Colombian Andes and Amazon Using Cloud-Computing. *International Journal of Applied Earth Observation and Geoinformation* **2022**, *107*, 102688, doi:10.1016/j.jag.2022.102688.
8. Rodríguez Eraso, N.; Armenteras-Pascual, D.; Retana Alumbreros, J. Land Use and Land Cover Change in the Colombian Andes: Dynamics and Future Scenarios. *Journal of Land Use Science* **2012**, 1–21, doi:10.1080/1747423X.2011.650228.
9. Calbi, M.; Clerici, N.; Borsch, T.; Brokamp, G. Reconstructing Long Term High Andean Forest Dynamics Using Historical Aerial Imagery: A Case Study in Colombia. *Forests* **2020**, *11*, doi:10.3390/f11080788.

10. Arrechea-Castillo, D.A.; Solano-Correa, Y.T.; Muñoz-Ordóñez, J.F.; Pencue-Fierro, E.L.; Figueroa-Casas, A. Multiclass Land Use and Land Cover Classification of Andean Sub-Basins in Colombia with Sentinel-2 and Deep Learning. *Remote Sensing* **2023**, *15*, doi:10.3390/rs15102521.
11. Gomez-Ossa, L.F.; Sanchez-Torres, G.; Branch-Bedoya, J.W. Land Cover Classification in the Antioquia Region of the Tropical Andes Using NICFI Satellite Data Program Imagery and Semantic Segmentation Techniques. *Data* **2023**, *8*, doi:10.3390/data8120185.
12. Franco, R.; Torres-Madronero, M.C.; Casamitjana, M.; Rondon, T. Spatial-Spectral Feature Extraction Using Multispectral Linear Unmixing for Land Use Land Cover Change Detection. *Journal of South American Earth Sciences* **2025**, *165*, 105722, doi:10.1016/j.jsames.2025.105722.
13. Murillo-Sandoval, P.J.; Hilker, T.; Krawchuk, M.A.; Hoek, J.V.D. Detecting and Attributing Drivers of Forest Disturbance in the Colombian Andes Using Landsat Time-Series. *Forests* **2018**, *9*, doi:10.3390/f9050269.
14. IDEAM *Actualización de Cifras de Monitoreo de La Superficie de Bosque - Año 2024. RESUMEN DE RESULTADOS DE MONITOREO*; Instituto de Hidrología, Meteorología y Estudios Ambientales - Ministerio de Ambiente y Desarrollo Sostenible: Bogota DC, Colombia, 2025;
15. Zhu, Z.; Woodcock, C.E. Continuous Change Detection and Classification of Land Cover Using All Available Landsat Data. *Remote Sensing of Environment* **2014**, *144*, 152–171, doi:10.1016/j.rse.2014.01.011.
16. Verbesselt, J.; Hyndman, R.; Newnham, G.; Culvenor, D. Detecting Trend and Seasonal Changes in Satellite Image Time Series. *Remote Sensing of Environment* **2010**, *114*, 106–115, doi:10.1016/j.rse.2009.08.014.
17. Armenteras, D.; Rodríguez, N.; Retana, J.; Morales, M. Understanding Deforestation in Montane and Lowland Forests of the Colombian Andes. *Reg Environ Change* **2011**, *11*, 693–705, doi:10.1007/s10113-010-0200-y.
18. Etter, A.; McAlpine, C.; Possingham, H. Historical Patterns and Drivers of Landscape Change in Colombia Since 1500: A Regionalized Spatial Approach. *Annals of the Association of American Geographers* **2008**, *98*, 2–23, doi:10.1080/00045600701733911.
19. Etter, A.; McAlpine, C.; Pullar, D.; Possingham, H. Modelling the Conversion of Colombian Lowland Ecosystems since 1940: Drivers, Patterns and Rates. *Journal of Environmental Management* **2006**, *79*, 74–87.
20. Le Saout, S.; Hoffmann, M.; Shi, Y.; Hughes, A.; Bernard, C.; Brooks, T.M.; Bertzky, B.; Butchart, S.H.M.; Stuart, S.N.; Badman, T.; et al. Protected Areas and Effective Biodiversity Conservation. *Science* **2013**, *342*, 803–805, doi:10.1126/science.1239268.
21. Hansen, M.C.; Potapov, P.V.; Moore, R.; Hancher, M.; Turubanova, S.A.; Tyukavina, A.; Thau, D.; Stehman, S.V.; Goetz, S.J.; Loveland, T.R.; et al. High-Resolution Global Maps of 21st-Century Forest Cover Change. *Science* **2013**, *342*, 850–853, doi:10.1126/science.1244693.
22. IDEAM Leyenda Nacional de Coberturas de la Tierra: Metodología CORINE Land Cover adaptada para Colombia. Escala 1:100.000 2010.
23. Stanimirova, R.; Tarrio, K.; Turlej, K.; McAvoy, K.; Stonebrook, S.; Hu, K.-T.; Arévalo, P.; Bullock, E.L.; Zhang, Y.; Woodcock, C.E.; et al. A Global Land Cover Training Dataset from 1984 to 2020. *Sci Data* **2023**, *10*, 879, doi:10.1038/s41597-023-02798-5.
24. Breiman, L. Random Forests. *Machine Learning* **2001**, *45*, 5–32, doi:10.1023/A:1010933404324.

25. Souza, C.M.; Roberts, D.A.; Cochrane, M.A. Combining Spectral and Spatial Information to Map Canopy Damage from Selective Logging and Forest Fires. *Remote Sensing of Environment* **2005**, *98*, 329–343, doi:10.1016/j.rse.2005.07.013.
26. Farr, T.G.; Rosen, P.A.; Caro, E.; Crippen, R.; Duren, R.; Hensley, S.; Kobrick, M.; Paller, M.; Rodriguez, E.; Roth, L.; et al. The Shuttle Radar Topography Mission. *Reviews of Geophysics* **2007**, *45*, doi:10.1029/2005RG000183.
27. Pekel, J.F.; Cottam, A.; Gorelick, N.; Belward, A.S. High-Resolution Mapping of Global Surface Water and Its Long-Term Changes. *Nature* **2016**, *540*, 418–422, doi:10.1038/nature20584.
28. Marconcini, M.; Metz-Marconcini, A.; Üreyen, S.; Palacios-Lopez, D.; Hanke, W.; Bachofer, F.; Zeidler, J.; Esch, T.; Gorelick, N.; Kakarla, A.; et al. Outlining Where Humans Live, the World Settlement Footprint 2015. *Sci Data* **2020**, *7*, 242, doi:10.1038/s41597-020-00580-5.
29. Arevalo, P.; Zhang, Y.; Friedl, M.A.; Woodcock, C.E.; Stanimirova, R.; Tarrio, K.; McAvoy, K.; Zhu, Z.; Bullock, E.; Gorelick, N.; et al. Global Land Cover Mapping and Estimation (GLanCE): A Record of Land Cover and Land Cover Change at Landsat Scale across Decades 2026.
30. Friedl, M.A.; Woodcock, C.E.; Olofsson, P.; Zhu, Z.; Loveland, T.; Stanimirova, R.; Arévalo, P.; Bullock, E.; Hu, K.-T.; Zhang, Y.; et al. Medium Spatial Resolution Mapping of Global Land Cover and Land Cover Change Across Multiple Decades From Landsat. *Frontiers in Remote Sensing* **2022**, *3*, doi:https://doi.org/10.3389/frsen.2022.894571.
31. Brown, J.F.; Tollerud, H.J.; Barber, C.P.; Zhou, Q.; Dwyer, J.L.; Vogelmann, J.E.; Loveland, T.R.; Woodcock, C.E.; Stehman, S.V.; Zhu, Z.; et al. Lessons Learned Implementing an Operational Continuous United States National Land Change Monitoring Capability: The Land Change Monitoring, Assessment, and Projection (LCMAP) Approach. *Remote Sensing of Environment* **2020**, *238*, 111356, doi:10.1016/j.rse.2019.111356.
32. Xian, G.Z.; Smith, K.; Wellington, D.; Horton, J.; Zhou, Q.; Li, C.; Auch, R.; Brown, J.F.; Zhu, Z.; Reker, R.R. Implementation of the CCDC Algorithm to Produce the LCMAP Collection 1.0 Annual Land Surface Change Product. *Earth System Science Data* **2022**, *14*, 143–162, doi:10.5194/essd-14-143-2022.
33. Abercrombie, S.P.; Friedl, M.A. Improving the Consistency of Multitemporal Land Cover Maps Using a Hidden Markov Model. *IEEE Transactions on Geoscience and Remote Sensing* **2016**, *54*, 703–713, doi:10.1109/TGRS.2015.2463689.
34. Cochran, W.G. *Sampling Techniques, 3rd Edition*; 3rd edition.; John Wiley & Sons: New York, 1977; ISBN 978-0-471-16240-7.
35. Olofsson, P.; Foody, G.M.; Herold, M.; Stehman, S.V.; Woodcock, C.E.; Wulder, M.A. Good Practices for Estimating Area and Assessing Accuracy of Land Change. *Remote Sensing of Environment* **2014**, *148*, 42–57, doi:10.1016/j.rse.2014.02.015.
36. Arévalo, P.; Baccini, A.; Woodcock, C.E.; Olofsson, P.; Walker, W.S. Continuous Mapping of Aboveground Biomass Using Landsat Time Series. *Remote Sensing of Environment* **2023**, *288*, 113483, doi:10.1016/j.rse.2023.113483.
37. Olofsson, P.; Arévalo, P.; Espejo, A.B.; Green, C.; Lindquist, E.; McRoberts, R.E.; Sanz, M.J. Mitigating the Effects of Omission Errors on Area and Area Change Estimates. *Remote Sensing of Environment* **2020**, *236*, 111492, doi:10.1016/j.rse.2019.111492.